2005

Chirp Slope Keying for Underwater Communications

Edit J. Kaminsky
University of New Orleans, ejbourge@uno.edu

Lastri Simanjuntak

Recommended Citation

Kaminsky, E. and L. Simanjuntak, "Chirp Slope Keying for Underwater Communications," in Proc. SPIE Sensors, and Command, Control, Communications, and Intelligence (C31) Technologies for Homeland Security and Homeland Defense IV Conf., Orlando, FL, 28 March-1 April, 2005, Vol. 5778, pp. 894-905. doi: 10.1117/12.605426

Chirp Slope Keying for Underwater Communications

Edit J. Kaminsky and Lastri Simanjuntak

Department of Electrical Engineering, University of New Orleans
New Orleans, LA 70148, U.S.A.

ABSTRACT

This paper presents a novel broadband modulation method for digital underwater communications: Chirp Slope Keying (CSK). In its simplest form, the binary information modulates the slope of a linear chirp, with up-chirps representing ones and down-chirps representing zeros. Performance evaluation in the form of probability of error vs. SNR show that the system performs as expected for AWGN environments and very well for more realistic models for underwater acoustical communications, such as the Raylegih channel with Doppler, delays, phase offset, and multipath.

Keywords: broadband, chirp modulation, underwater, communications

1. INTRODUCTION

This paper presents a novel and robust system for spread spectrum acoustical underwater communications: chirp slope keying (CSK). Digital modulation schemes are based on the message modulating the amplitude, as in ASK, the phase, as in PSK, the frequency of the carrier, as in FSK, or combinations of these. In the simplest form of CSK, the digital modulating data are represented by the slope of a linear chirp signal, where an up chirp (i.e., increasing frequency) represents a "1" and a down chirp (decreasing frequency) represents a "0". Higher dimensional constellations are easily obtained by using a larger number of up/down slopes. Due to the wide bandwidth in CSK, immunity against various frequency selective impediments may be expected.

CSK, as all spread spectrum systems, utilizes a data modulated signal which has its energy spread over a bandwidth which is much greater than the rate of information being sent; the selective fading problem is reduced by using broadband signals. Simulations demonstrate that even with the simplest receiver, CSK offers sturdy performance in the modeled ocean environment. The purpose of the work reported here is to introduce and evaluate this modulation method. We present an overview of chirp-slope keying and demodulation methods as well as the performance evaluation in AWGN and Rayleigh amplitude fading channels with various deleterious multipath effects. This coherent scheme is proposed for wireless underwater acoustical communications where current transmission rates and performance have enormous room for improvement.[1]

Establishing communication between two remote underwater sites by using cable connected between a receiver and a transmitter, even if possible, has several disadvantages: it is expensive, maintenance and repair are difficult especially if the communication takes place in the deep water, and the drag from the cable can be a problem if the user is small and mobile. The alternative is to use sound propagated through water: the underwater acoustic (UWA) channel. From a communication perspective, the UWA channel poses many challenges to the realization of reliable, high data rate, and long distance communications, because it is quite possibly nature's most unforgiving wireless communication medium.

Modeling the underwater channel accurately has a very important role in obtaining proper characterization of communications systems. Much recent work has focused on channel characterization and modeling[2-5] There are four aspects of the UWA channel that are of primary concern: ambient noise, transmission loss due to geometrical spreading and absorption, reverberation due to multipath, and Doppler spreading due to relative motion. Each must be considered in modeling the appropriate UWA channel[6-8].

E-mail: ejbourge@uno.edu, Telephone: 1 504 280 5616

Sensors, and C3I Technologies for Homeland Security and Homeland Defense IV, edited by Edward M. Carapezza, Proceedings of SPIE Vol. 5778 (SPIE, Bellingham, WA, 2005) · 0277-786X/05/$15 · doi: 10.1117/12.605426

Ambient noise is caused by man-made activities, sea life, and waves. The noise levels are site-dependent, especially in shallow water. Ambient noise influences the signal-to-noise ratio which ultimately constrains the data transmission rate for a given probability error or decreases accuracy for a given rate. Transmission loss is caused by energy spreading and sound absorption. The absorption loss occurs due to energy lost to heat in the water. This loss increases with both frequency and range. It is a primary factor in determining the maximum usable frequency, hence the available bandwidth for a particular range. The most challenging aspect of the UWA channel is the reverberation due to multipath propagation. The mechanism of multipath formation is dependent on the location and depth within the ocean and on the frequency and range of transmission. Two main mechanisms of multipath formation are the reflection at the water boundaries (bottom, surface, and any objects in the water), and ray bending. Multipath propagation contributes to signal fading, and causes inter-symbol interference (ISI) in digital communication systems. In the past, this multipath propagation resulted in restricting communication in the UWA channel to noncoherent modulation schemes, and low data rates.[6] Doppler spreading is one implication of relative motion between the transmitter and receiver or by ocean internal factors (such as water motion in the channel). Some motion can be compensated for, e.g. if the motion is slowly varying due to ship travel. However, random motion manifests a continuous spreading that is more difficult to compensate for.

For decades, underwater acoustics have received much attention, mostly by the military, associated with submarines detection. In recent years, the applications of underwater acoustic communications are beginning to shift towards commercial applications. These systems are now employed in various unmanned submersibles which are replacing divers in a variety of offshore work tasks.

For high data rates on time-spread multipath propagation channels, one approach to signal design which avoids the effects of multipath is the use of frequency shift keying (FSK) or phase shift keying (PSK).[9] Non-coherent demodulation has generally been preferred recently because of the phase instabilities caused by the Doppler spreading.[10,11] Spread spectrum techniques are being considered for resolving these problems[12] because spread spectrum can make effective use of bandwidth and tolerate large distortion. This includes the chirp-slope keying (CSK) digital modulation scheme discussed in this paper. Spread spectrum signals resist multipath, decorrelate impulsive noise, resist jamming interference, and provide some immunity to frequency selective fading.

The rest of this paper is organized as follows: Section 2 presents the chirp slope keying scheme. The simple channel models used in this paper are discussed in Section 3. Simulation strategies are discussed in Section 4 and performance evaluation and simulation results are given in Section 5. Concluding remarks and suggestions for further work are presented in Section 6, followed by references.

2. CHIRP-SLOPE KEYING

Analog chirp signals or linear frequency modulation signals have been used extensively in radar technology and, more recently, in sonar systems. Linear chirp signals –known as linear frequency modulation (linear-FM)– have been used in radar technology since the mid-1940s. Chirp modulation is one of the older spread spectrum methods.[13,14] The basic idea is to transmit long frequency modulated pulses in which the frequency changes continuously in one direction (increasing or decreasing) without reversal for the duration of the pulse. Chirp signals in digital communications were seemingly originally suggested by Winkler in 1962.[15] A pair of linear chirps that have opposite chirp rates are used for binary signaling. The chirps we consider here are of constant amplitude, but Gaussian chirps or raised-cosine tapered chirps are also common. The chirps have a symbol duration of T. Within this time, the frequency is rising or falling monotonically. The difference between the lower and upper frequency approximately represents the bandwidth of the pulse. Binary chirp signalling, called linear frequency sweeping (LFS) by Berni,[16] is compared to FSK and PSK in coherent, partially coherent, and fading channels (Rayleigh and Rician channel models). Berni found that LFS is superior to FSK with 1.3 dB improvement in terms of required signal energy and bandwidth for a given probability of error in coherent channels. In non-coherent channels, LFS is less appealing because of the requirement for a phase recovery system. In non-selective slow fading channels, the relatively simpler implementation of FSK rules out the use

of LFS for orthogonal signaling. However, chirp signals have superior characteristics in the partially coherent and fading cases, for certain ranges of channel conditions.

The use of chirp modulation for multiple access with chirp signals hopping different modulation slopes and different bandwidths, was first proposed by Cook[17] in 1974. El-Khamy extended Cook's approach to improve performance[18-21]. In 2002, Hengstler[22] extended Cook's and El-Khamy's approach for efficient and flexible multiple access using the new chirp modulation spread spectrum (CMSS). Hengstler's CMSS outperforms direct sequence spread spectrum systems.

In recent years, more authors have researched and utilized chirp signals in communications systems. A chirp FSK modem for high reliability communications in shallow water was presented by Leblanc.[23] Fifty six narrowband chirp FSK pulses, each centered at a unique frequency in the range of 20 KHz to 30 KHz, were used. The communication rates varied from 300 bps to 2400 bps. An improved modem[24] uses 56 narrowband chirp FSK pulses, each centered at a unique frequency in the range of 16 KHz to 32 KHz with rates from 221 to 1172 bps. Experiments showed that the system is virtually insensitive to selective fading, reverberation, and Doppler.

In this paper, simple linear down and chirp signals are used to represent binary 0 and 1, respectively. Simulations show that even with only a first order filter at the receiver, the system shows an excellent performance in the worst channel for certain ranges of signal-to-noise ratios (SNR). Our system may be easily expanded to represent higher order modulation by increasing the number of up and down chirps, i.e., using a larger number of slopes.

A linear complex chirp signal may be modeled as:

$$S_c(t) = \exp\left[j(2\pi f_0 t + \pi\mu t^2)\right] \tag{1}$$

where f_0 is the carrier frequency and μ is the chirp rate. In terms of maximum and minimum frequencies, $f_{\max}$ and $f_{\min}$, an up chirp is represented as in (2), while a down chirp is represented by (3):

$$S_{cu}(t) = \exp\left[2\pi j t\left(\frac{f_{\max} - f_{\min}}{T}t + f_{\min}\right)\right] \tag{2}$$

$$S_{cd}(t) = \exp\left[2\pi j t\left(\frac{f_{\min} - f_{\max}}{T}t + f_{\max}\right)\right] \tag{3}$$

The one-dimensional real chirps are obtained by replacing the complex exponentials by their real parts:

$$S(t) = \mathrm{Re}\{S_c(t)\} \qquad S_u(t) = \mathrm{Re}\{S_{cu}(t)\} \qquad S_d(t) = \mathrm{Re}\{S_{cd}(t)\} \tag{4}$$

The CSK scheme, then, works as follows: the binary stream $\{b_i(n)\}$ selects the chirp pulses $\{S_n(t)\}$ to be transmitted at each signalling interval based on its value:

$$s_n(t) = \begin{cases} S_u(t), & b_i = 1 \\ S_d(t), & b_i = 0 \end{cases}, \quad nT \le t \le (n+1)T \tag{5}$$

3. UNDERWATER CHANNEL MODELS

In order to be able to perform underwater acoustic communication, it is important to understand what happens to the signal on its way from the transmitter to the receiver; knowledge of the physical properties of the underwater medium is crucial and plays a key role in designing communication systems. Very simple models will be used here to simulate the UWA channel's ambient noise, transmission loss due to geometrical scattering and absorption, reverberation due to multipath, and Doppler spreading due to relative motion.

Due to the random nature of the underwater media statistical models are used to model the AUW channel for simulation of communications systems. Many researchers use the Additive White Gaussian Noise (AWGN) to model the ambient noise in underwater channels.[2,5,10,11,22] In some cases, authors also use the Gaussian distribution to model the phase shift or the time delay.[2] Some authors believe that the delay and the phase shift are stable enough that they can be considered to be deterministic[3]; we follow this approach. Due to fading multipath characteristics of the underwater channel, many researches have preferred to model the underwater channel using non-Gaussian models. Some, as we do, believe that the channel amplitude response can be modeled by a Rayleigh distribution[2,25] although there are still disagreements.[4]

3.1. Additive White Gaussian Noise (AWGN) Channel

The fundamental communication channel, the Additive White Gaussian Noise channel (AWGN), is chosen as the first channel model for our simulations. There are three facts about the Gaussian density which contribute to its wide use and success in representing most communication channel models[26]: Many physical processes are indeed Gaussian, the central limit theorem, and the fact that linear systems preserve Gaussianity.

The signal s(t) is transmitted through the AWGN underwater channel. The received signal r(t) can be modeled as:

$$r(t) = s(t) + n_g(t) \tag{6}$$

where $n_g(t)$ is the zero-mean Gaussian random process. The signal-to-noise ratio (SNR) is defined as

$$\text{SNR (dB)} = 10\log_{10}\frac{E_s}{E_n} \tag{7}$$

with E_s as the signal energy in one symbol $s(t)$ and E_n is the double sided energy of the white Gaussian noise process, given as:

$$E_n = 2W\sigma_g^2 \tag{8}$$

where W is defined as the channel bandwidth and σ_g^2 is the variance of the AWGN.

For a linear chirp signal with slopes $\pm\mu$, the power is:

$$E_s = \frac{1}{T}\int_{-T/2}^{T/2}\cos^2(2\pi ft \pm \mu t^2)dt \tag{9}$$

which yields Fresnel integrals. With the assumption that the arguments of $C_f(x)$ and $S_f(x)$ are large numbers, the power of the linear chirp can be approximated to be just above 1/2.

3.2. Rayleigh Fading Channel

In this model, a time-varying, multiplicative amplitude scaling, $A_r(t)$, is used to model the amplitude attenuation. $A_r(t)$ is the Rayleigh fading random process with probability density function (PDF) at time t given by

$$f_r(A) = \begin{cases} \frac{A}{\sigma^2} \exp\left(\frac{-A^2}{2\sigma^2}\right), & A > 0 \\ 0, & A \leq 0 \end{cases} \tag{10}$$

The mean and the variance of the Rayleigh distribution with parameter σ are, respectively:

$$\mu_r = \sigma\sqrt{\frac{\pi}{2}}; \qquad \sigma_r^2 = \left(2 - \frac{\pi}{2}\right)\sigma^2 \tag{11}$$

The channel capacity in a Rayleigh fading channel is always lower than that in a Gaussian noise channel. The capacity of a Rayleigh fading channel is reduced by 32% from the Gaussian channel at SNR = 10 dB, and reduced by 11% at SNR = 25 dB.[27]

In this case we define our signal-to-noise ratio as:

$$\text{SNR (dB)} = 10\log_{10}\frac{E_{Rs}}{E_n} \tag{12}$$

where E_{Rs} is the average energy in one faded symbol:

$$E_{Rs} = E\left\{[A_r(t)s(t)]^2\right\} \tag{13}$$

with $A_r(t)$ the Rayleigh amplitude. The SNR of (12) can therefore be rewritten as

$$\text{SNR}(dB) = 10\log_{10}\frac{2\sigma^2 E_s}{E_n} \tag{14}$$

with σ the Rayleigh parameter in (10) and E_n the double sided power of the white Gaussian noise defined in (8). E_s is still given, as before, by (9).

4. CSK SIMULATIONS

The digital information to be transmitted using CSK is contained in the slope of the chirp's signal. This section briefly discusses several receiver structures that could be used to detect the linear frequency slope of the chirp signal. However, the only structure we actually simulate and evaluate is the sub-optimal integrate-and-dump detector. We expect some other receivers to perform better, especially when phase delays, time delays, and Doppler are present.

The integrate-and-dump detector is the simplest implementation of the receiver. It first performas a multiplication by a chirp and then it integrates the product over a period interval and thresholds the result to determine the binary information sequence.

A matched filter may also be used at the receiver. The matched filter maximizes the signal-to-noise ratio (SNR) and minimizes the probability of error in AWGN.

Another possible detector structure is one that determines the slope of the frequency sweep by using a line detection method such as the Hough Transform. The same technique can be used to detect the frequency slope of the chirp signal. Hough Transform can easily distinguish between the up- and down-chirp even when the signal is highly distorted.

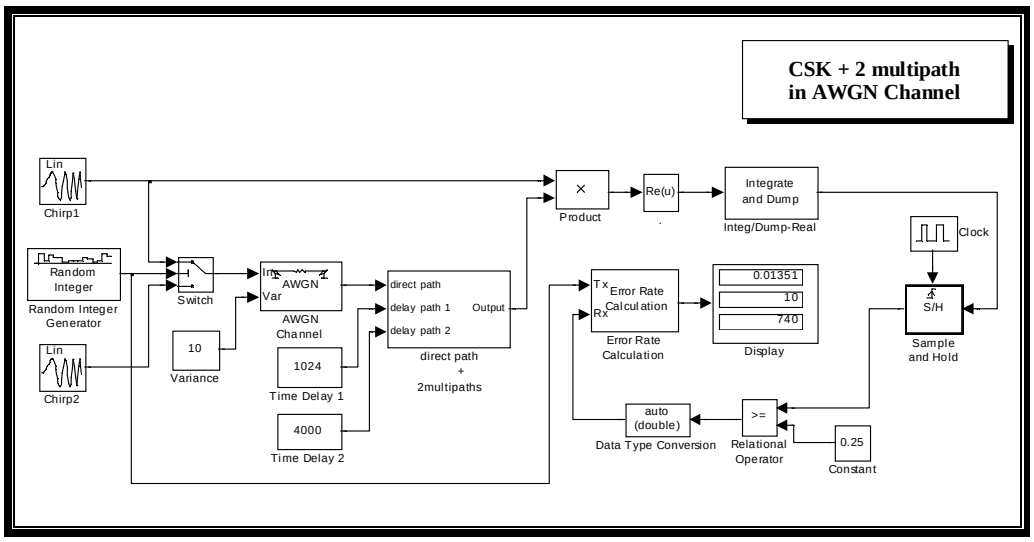

Figure 1: Block diagram of simulated CSK system in AWGN channel.

Table 1: CSK simulation parameters

Parameter	Value
Symbol rate	1 s
Sampling rate	512 samples/s
f_{min}	25 Hz
f_{max}	125 Hz
Chirp rate (slope)	100 Hz/s

The proposed detection for our CSK employs the integrate-and-dump correlation detector. It is basically identical to standard BPSK receiver already in operation which could be directly used by changing only the signal into the receiver's multiplier. A random binary number generator block creates equally likely binary digits. The chirp signal generator block generates the linear-up-chirp signal ("1") and the linear-down-chirp signal ("0"). Fig. 1 depicts the entire CSK modulation and demodulation process in the additive white Gaussian noise channel with multipath. All simulations were implemented using Matlab's Simulink 5*.

Fig. 2 depicts details of the multipath block, clearly showing the addition of two delayed, amplitude scaled, phase- and frequency- shifted signals to the direct path signal. The parameters used in the simulations are given in Table 1.

At the receiver, the signal is demodulated by multiplying the received signal with another up-chirp, $S_u(t)$. This operation is performed by the chirp-up and product blocks. The products, when no interfering signals are present, are given in (15) and (16) for a treansmitted up ("1") or down ("0") chirp, respectively:

$$y_u(t) = \frac{1}{2} + \frac{1}{2}\left[\cos\left(4\pi f_{\min} t\right)\cos\left(2\pi t^2\right) - \sin\left(4\pi f_{\min} t\right)\sin\left(2\pi t^2\right)\right] \tag{15}$$

$$y_d(t) = \frac{1}{2}\left[\cos\left(2\pi\left(f_{\max} - f_{\min}\right)t\right)\cos\left(2\pi t^2\right) + \sin\left(2\pi\left(f_{\max} - f_{\min}\right)t\right)\sin\left(2\pi t^2\right) + \cos\left(2\pi\left(f_{\max} + f_{\min}\right)t\right)\right] \tag{16}$$

*Matlab and Simulink are trademarks of The Mathworks.

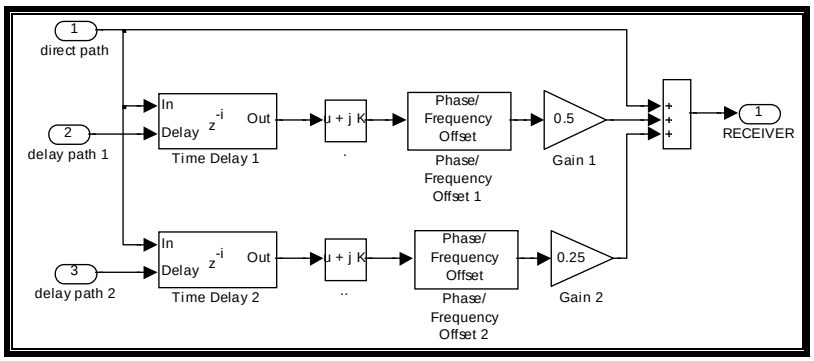

Figure 2: Details of the multipath block.

By applying a first order low pass filter (LPF) to the system with a cutoff frequency of much less than 2πB and $4\pi f_{min}$ ($f_c \ll 2\pi$B and $4\pi f_{min}$), leaves approximately only the DC term. The filtered signals, y_{fu} and y_{fd} are given by

$$y_{fu}(t) = \text{LFP}\left\{y_u(t)\right\} \approx \frac{1}{2}; \qquad y_{fd}(t) = \text{LFP}\left\{y_d(t)\right\} \approx 0 \tag{17}$$

By setting a threshold at the mid-point, 1/4, the binary sequence b_i can be recovered. For all $y(t) \geq 1/4$, the binary data is assigned a value of 1, and for all $y(t) < 1/4$, it is demodulated as zero. In order to determine the "no data present" condition and distinguish this from the down chirp, two rails could be use with the top rail as described above, and the lower rail performing a multiplication by a down chirp. The thresholding would then be replaced by a comparator with the largest indicating the 'winner' and producing the binary output. The resulting signal is then integrated at the integrate-and-dump block, essentially performing a simple, first order low pass filter. This block integrates the input signal in discrete time and resets to zero every period T. The sample-and-hold block acquires $y(t)$ whenever it receives a trigger from the clock and holds the value for a whole period. Because the output of the sample-and-hold block has to wait for a whole period, the demodulated data is delayed by T.

Both AWGN and Rayleigh fading channels were used to model the UWA channel. In both cases, simple ISI interference (multipath) was also included. The interfering signals were scaled (α) and shifted in time (τ), frequency (υ) and phase (φ). The overall signal at the output of the channel (input to receiver) is:

$$r(t) = r_0(t) + r_1(t + \tau_1, \varphi_1, f + \upsilon_1) + r_2(t + \tau_2, \varphi_2, f + \upsilon_2) \tag{18}$$

where without multipath the signal is

$$r_0(t) = \cos(2\pi f_0 t \pm \pi\mu t^2) + n_g(t)$$

with chirp rate μ and Gaussian noise n_g. The multipath interfering signals are

$$r_i(t) = \alpha_i \cos\left[2\pi(f_0 + \upsilon_i)(t + \tau_i) \pm \pi\mu(t + \tau_i)^2 + \varphi_i\right]$$

The multipath simulation parameters are given in Table 2, and include delay in time, τ, shift in phase, φ, and shift in frequency, υ. For simplicity, these parameters are constant throughout our simulations.

Table 2: Multipath parameters

	Multipath 1	Multipath 2
Time delay, τ	2 T	7.8 T
Freq shift, υ	20 Hz	50 Hz
Phase shift, φ	30°	20°
Scaling, α	-3 dB	-6 dB

5. RESULTS

Performance evaluation of CSK was performed over two different underwater channel models, each with and without multipath ISI.

The simple AWGN model is expanded by introducing the Rayleigh amplitude fading, $A_r(t)$. The last subsection compares the performance over all channels, as well as to the performance of binary phase shift keying (BPSK).

The simulated BER curves were obtained by computing the probability of error after at least 10 bits errors, for each SNR value.

5.1. Simulation over AWGN channel

The first channel modeled is the standard Additive White Gaussian Noise (AWGN). The system achieves a BER of 10^{-3} with an SNR of 13 dB. To the above AWGN channel we added multipath, where two delayed and scaled versions of the transmitted signal are added to the message-conveying waveform. The interfering signals are shifted both in time and frequency (Doppler) and contain a shift in phase, resulting in a received signal spread in time and frequency. The system is able to achieve a BER of 10^{-3} with an SNR of 15 dB, a 2 dB degradation from the performance in AWGN alone.

5.2. Simulations with Rayleigh Amplitude Fading

The next channel modeled has AWGN and Rayleigh amplitude fading:

$$r(t) = A_r(t)s(t) + n_g(t) \tag{19}$$

where again $n_g(t)$ is the Gaussian noise and $A_r(t)$ represents the Rayleigh fading. We used two different values of the fading parameter, σ. With $\sigma = 1$, the system is able to achieve a BER of 10^{-3} with an SNR of 15 dB. For SNR smaller than about 11 dB, the Rayleigh parameter value does not influence the average BER.

The SNR is defined as in 12 with E_s the energy of s_u or s_d and the energy of Rayleigh fading of approximately -3 dB for $\sigma = 1$, and about -8 dB for $\sigma = 0.5$.

The last, most complex, and probably most realistic channel model includes additive white Gaussian noise, Rayleigh fading, and also multipath (two delayed signals added to the direct path):

$$r(t) = A_r(t)\left[r_0(t) + r_1(t+\tau_1, \varphi_1, f+\upsilon_1) + r_2(t+\tau_2, \varphi_2, f+\upsilon_2)\right] + n_g(t) \tag{20}$$

Even in this deleterious channel, the system is able to achieve a BER of 10^{-3} with an SNR of 16.5 dB with $\sigma = 1$ for the Rayleigh parameter. The Rayleigh parameter σ influences the performance only for SNR above 14 dB.

Table 3: Performance of CSK in various channels

Channel	SNR for BER = 10^{-3}	SNR BER =10^{-6}
AWGN	13 dB	17 dB
AWGN + Multipath	15 dB	19.2 dB
AWGN + Rayleigh Fading	15 dB	19.7 dB
AWGN + Rayleigh Fading + Multipath	16.5 dB	20.7 dB

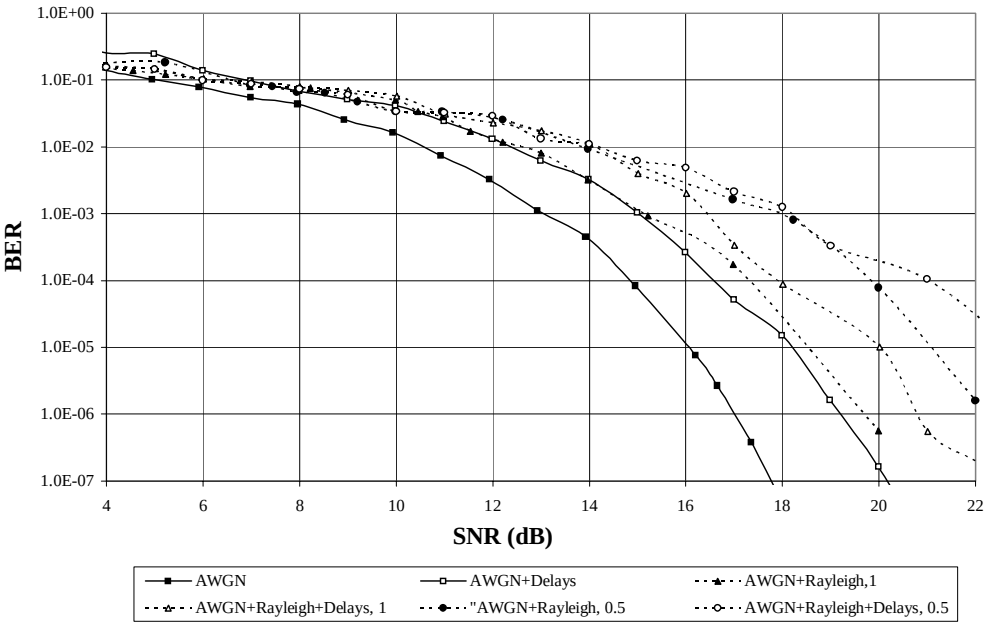

Figure 3: Performance of CSK in terms of probability of error vs SNR for all channels investigated.

5.3. Comparison of all Results

To complete the presentation of simulation results, we compare and discuss all results. The BER curves for all channel models together are shown in Figure 3. The pink line curve is for the channel with AWGN only, the most benign channel. The blue line curve is for the channel with the Gaussian noise and multipath signals. The curve in red is for the channel with the Gaussian noise and the Rayleigh fading with Rayleigh parameter of $\sigma = 1$. The last curve in green is the channel with Gaussian noise, Rayleigh fading ($\sigma = 1$), and multipath signals. The BER and SNR values of these four channel models are listed in Table 3, for two significant values of BER. In all cases the solid lines are for the channels without ISI while the dashed lines correspond to the signals with two indirecy paths, delayed in phase, frequency, and phase, as discussed before. the squares represent the AWNG channel while the triangles ($\triangle$) are for Rayleigh fading with $\sigma = 1$ and the upside down triangles (∇) are for Rayleigh parameter $\sigma = 0.5$.

Overall, the performance in AWGN degrades by about 2 dB when delays are included to represent multipath for BER of 10^{-3}. When Rayleigh fading is present, the SNR ration must be increased by approximately 1.5 dB to counteract the effects of the ISI interference. By introducing Rayleigh fading, the BER performance degrades by approximately 2 dB, so the effect of the Doppler and the Rayleigh fading contribute the same degradation to the AWGN channel.

Fig. 4 compares the BER performance of CSK and BPSK in the AWGN and Rayleigh amplitude fading channels. Both modulation schemes utilize the same demodulation method. The solid lines are results for CSK

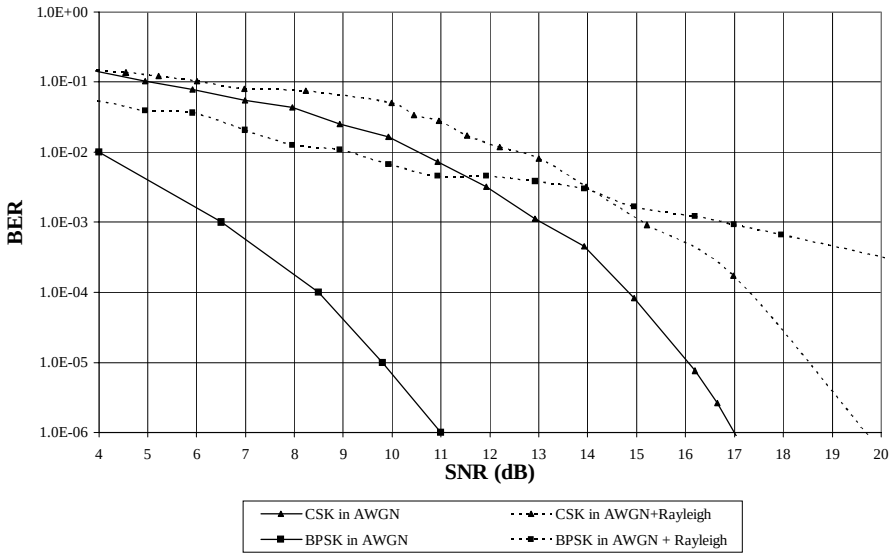

Figure 4: Comparison of CSK to BPSK.

and the dashed lines are for BPSK.

In AWGN channel, the graph shows the performance of CSK is worse than BPSK by approximately 6 dB for BER of 10^{-3}, as expected. The output of the integrate-and-hold for BPSK is either + $\frac{1}{2}$ or - $\frac{1}{2}$ for data of 1 or 0 respectively, whereas the output for CSK is either + $\frac{1}{2}$ or 0 for data 1 or 0, respectively. There is $\frac{1}{2}$ difference in magnitude, or 6 dB difference in power. However, when Rayleigh amplitude fading is present, CSK is more desirable because the BPSK performance degrades more than CSK does. The performance opf CSK is almost 4 dB better than BPSK at BER of 10^{-4} and about 2 dB at 10^{-3}. This improvement is expected to be more drastic when better receivers are used.

5.4. Sampling rate and Lowpass filter

Choosing the sampling rate proved to be a difficult task. We can see from Fig. 5 that the BER obtained in our simulations depends on the sampling rate (always above Nyquist rate). As we increased the sampling rate, the BER was reduced. By increasing the sampling rate from the Nyquist rate to 512 samples per period, on average, the BER improves approximately by 36%; and when increased from 512 samples per period to 1024 samples per period, the BER improves approximately by and additional 42%. The BER values depicted in Fig. 5 are obtained from the AWGN channel with SNR of 7 dB.

6. CONCLUSIONS AND SUGGESTIONS FOR FURTHER WORK

We have presented a discussion of a digital modulation method using Chirp Slope Keying (CSK) for coherent underwater acoustic communications. By implementing a first order filter with an integrate-and-dump at the receiver, we showed good quality of detection of the transmitted binary signal. The system was simulated in four different statistical underwater channel models. These channel models consisted of the additive white Gaussian noise, the Rayleigh fading, and multipath signals with shifts in time, phase, and frequency. The BER curves versus SNR were presented and clearly demonstrate the feasibility of CSK for digital transmission underwater. Many of the multipath parameters (the time shift, phase shift, frequency shift, and gain) used in this paper were chosen somewhat arbitrarily. Randomization of these parameters, using appropriate distributions will create a more realistic channel model and more accurate average performance characterization. Experimental data

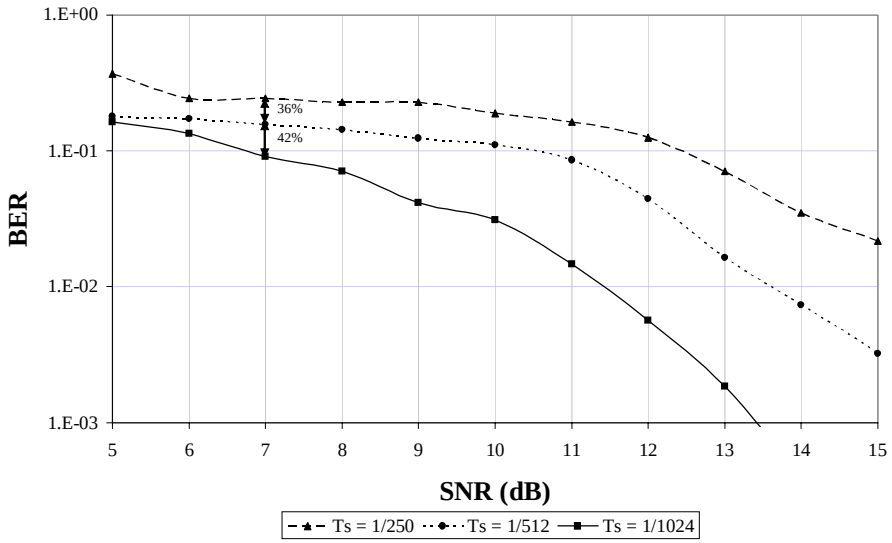

Figure 5: Performance of CSK in AWGN with different sampling rates.

needs to be collected to validate the channel models; this should include measurement of Doppler spread in realistic situations.

The performance of any communication system is heavily dependent on the internal and external synchronizations. We assumed that both synchronizations are achieved without error. However, this assumption is unrealistic. So another possible future research area would concentrate on determining the degradation of the system performance due to synchronization errors.

A larger improvement of binary CSK over other standard digital modulation schemes is expected as channel conditions deteriorate. PSK is very sensitive to phase shift and Rayleigh amplitude. FSK is extremely sensitive to frequency shift and frequency selective fading. ASK cannot handle amplitude fading. Even though CSK is about 6 dB worse in the most benign AWGN channel, this deficit decreases as channel conditions worsen. CSK outperforms others in these very deleterious channels, for high SNR.

A very simple integrator is used as the LPF in the demodulator. Implementing different receiver configurations can easily improve the performance of CSK systems. These receiver configurations may include matched filtering receiver or frequency slope detection receiver using, for example, the Hough Transform.

Expanding Binary CSK to Quadrature CSK (QCSK) for transmission at 2 bits/sec/Hz can easily be done by doubling the number of available slopes in the chirps; this doubles the number of bits transmitted per signaling interval. CSK can also be extended to M-ary CSK for transmission at $\log_2(M)$ bits/sec/Hz to more efficiently utilize the available bandwidth.

REFERENCES

1. D. B. Kilfoyle, J. C. Preisig, and M. Stojanovic, "Special issue on underwater acoustic communications," *IEEE Transactions on Oceanic Engineering* **25**, January 2000.
2. D. B. Kilfoyle and A. B. Baggeroer, "The state of the art in underwater acoustic telemetry," *IEEE Journal of Oceanic Engineering* **25**, pp. 4–27, January 2000.
3. A. Essebbar, G. Loubet, and F. Vial, "Underwater acoustic channel simulations for communication," in *Proc. IEEE Oceans'99*, *IEEE Oceans* **3**, pp. 495–500, September 1994.

4. D. Middleton, "Channel modeling and threshold signal processing in underwater acoustics: An analytical overview," *IEEE Journal of Oceanic Engineering* **OE-12**, pp. 4–28, January 1987.
5. H. V. Poor, "Uncertainty tolerance in underwater acoustic signal processing," *IEEE Journal of Oceanic Engineering* **OE-12**, pp. 48–65, January 1987.
6. M. Stojanovic, "Underwater acoustic communications," *IEEE Electro International* , pp. 435–440, June 1995.
7. W. S. Burdic, *Underwater Acoustic System Analysis*, Prentice Hall, 1991.
8. A. B. Baggeroer, "Acoustic telemetry –An overview," *IEEE Journal of Oceaninc Engineering* **OE-9**, pp. 229–235, October 1984.
9. M. Johnson, J. Preisig, L. Freitag, and M. Stojanovic, "FSK and PSK performance of the utility acoustic modem," in *Proc. Oceans 1999*, pp. 1512–1515, MTS/IEEE, September 1999.
10. T. Eggen, A. Baggeroer, and J. Preisig, "Communication over doppler spread channels –Part I: Channel and receiver presentation," *IEEE Journal of Oceanic Engineering* **25**, pp. 62–71, January 2000.
11. T. Eggen, A. Baggeroer, and J. Preisig, "Communication over doppler spread channels –Part II: Receiver characterization and practical results," *IEEE Journal of Oceanic Engineering* **26**, pp. 612–621, October 2001.
12. R. C. Dixon, *Spread Spectrum Systems*, Wiley-Interscience, 1976.
13. J. Holmes, *Encyclopedia of Science and Technology*, vol. 17, ch. Spread Spectrum Communication, pp. 271–273. McGraw-Hill, 8 ed., 1997.
14. J. R. Klauder, A. C. Price, S. Darlington, and W. J. Albersheim, "The theory and design of chirp radars," *Bell Syst. Tech. Journal* **39**, pp. 745–808, 1960.
15. M. R. Winkler, "Chirp signals for communications," in *WESCON Convention Record*, p. Paper 14.2, 1962.
16. A. J. Berni and W. D. Greeg, "On the utility of chirp modulation for digital signaling," *IEEE Transactions on Communications* **21**, pp. 748–751, June 1973.
17. C. E. Cook, "Linear FM signal formats for beacon and communication systems," *IEEE Transactions on Aerospace and Electronic Systems* **AES-10**, pp. 471–478, July 1974.
18. S. E. El-Khamy, S. E. Shaaban, and E. A. Thabet, "Partially coherent detection of continuous phase chirp (CPCM) signals," in *Proc. Thirteenth National Radio Science Conference*, pp. 485–495, March 1996.
19. S. E. El-Khamy, S. E. Shaaban, and E. A. Thabet, "Multi-user chirp modulations signals (M-CM) for efficient multiple-access communication systems," in *Proc. Thirteenth National Radio Science Conference*, pp. 289–297, March 1996.
20. S. E. El-Khamy and S. E. Shaaban, "Efficient multiple access communications using multi user chirp modulation signals," in *Proc. 4th IEEE International Symposium on Spread Spectrum Techniques and Applications*, **3**, pp. 1209–1213, IEEE, September 1996.
21. S. E. El-Khamy, S. E. Shaaban, and E. A. Thabet, "Frequency-hopped multi-user chirp modulation (FH/M-CM) for multiple fading channels," in *Proc. Sixteenth National Radio Science Conference*, pp. C6/1–C6/8, 1999.
22. S. Hengstler, D. P. Kasilingam, and A. H. Costa, "A novel chirp modulation spread spectrum technique for multiple access," in *Proceedings of the IEEE International Symposium on Spread Spectrum Techniques and Applications*, **1**, pp. 73–77, September 2002.
23. L. R. Leblanc, P. Beaujean, M. Singer, C. Boubli, and G. T. Strutt, "Chirp FSK modem for high reliability communication in shallow water," in *Proc. Oceans 1999*, **1**, pp. 222–227, IEEE/MTS, September 1999.
24. L. R. Leblanc, M. Singer, P. Beaujean, C. Boubli, and J. R. Alleyne, "Improved chirp FSK modem for high reliability communications in shallow water," in *Proc Oceans 2000*, **1**, pp. 601–603, MTS/IEEE, September 2000.
25. G. Cook and A. Zaknich, "Chirp sounding the shallow water acoustic channel," in *Proceedings of the 1998 IEEE International Conference on Acoustics, Speech, and Signal Processing*, **4**, pp. 2521–2524, May 1998.
26. R. N. McDonough and A. D. Whalen, *Detection of Signals in Noise*, Academic Press, 1995.
27. W. C. Lee, "Estimate of channel capacity in rayleigh fading environment," *IEEE Transactions on Vehicular Technology* **39**, pp. 187–189, August 1990.